Antitumor Activity of the Novel BTK Inhibitor TG-1701 Is Associated with Disruption of Ikaros Signaling in Patients with B-cell Non–Hodgkin Lymphoma

Marcelo Lima Ribeiro[1,2], Diana Reyes-Garau[1], Meritxell Vinyoles[3,4,5], Núria Profitós Pelejà[1], Juliana Carvalho Santos[1], Marc Armengol[1,6], Miranda Fernández-Serrano[1,6], Alícia Sedó Mor[1,6], Joan J. Bech-Serra[7], Pedro Blecua[8], Eva Musulen[8,9], Carolina De La Torre[7], Hari Miskin[10], Manel Esteller[5,8,11], Francesc Bosch[6,12,13], Pablo Menéndez[3,4,5,11], Emmanuel Normant[10], and Gaël Roué[1,6,12,13]

ABSTRACT

Purpose: Despite the remarkable activity of BTK inhibitors (BTKi) in relapsed B-cell non–Hodgkin lymphoma (B-NHL), no clinically-relevant biomarker has been associated to these agents so far. The relevance of phosphoproteomic profiling for the early identification of BTKi responders remains underexplored.

Experimental Design: A set of six clinical samples from an ongoing phase I trial dosing patients with chronic lymphocytic leukemia (CLL) with TG-1701, a novel irreversible and highly specific BTKi, were characterized by phosphoproteomic and RNA sequencing (RNA-seq) analysis. The activity of TG-1701 was evaluated in a panel of 11 B-NHL cell lines and mouse xenografts, including two NF-κB- and BTK^{C481S}-driven BTKi-resistant models. Biomarker validation and signal transduction analysis were conducted through real-time PCR, Western blot analysis, immunostaining, and gene knockout (KO) experiments.

Results: A nonsupervised, phosphoproteomic-based clustering did match the early clinical outcomes of patients with CLL and separated a group of "early-responders" from a group of "late-responders." This clustering was based on a selected list of 96 phosphosites with Ikaros-pSer442/445 as a potential biomarker for TG-1701 efficacy. TG-1701 treatment was further shown to blunt Ikaros gene signature, including *YES1* and *MYC*, in early-responder patients as well as in BTKi-sensitive B-NHL cell lines and xenografts. In contrast, Ikaros nuclear activity and signaling remained unaffected by the drug *in vitro* and *in vivo* in late-responder patients and in BTK^{C481S}, BTK^{KO}, and noncanonical NF-κB models.

Conclusions: These data validate phosphoproteomic as a valuable tool for the early detection of response to BTK inhibition in the clinic, and for the determination of drug mechanism of action.

Introduction

B-cell non–Hodgkin lymphomas (B-NHL) account for up to 4% of globally diagnosed cancers (1). They are divided into low and high grades, typically corresponding to indolent (slow-growing) lymphomas, like chronic lymphocytic leukemia (CLL), and aggressive lymphomas, like diffuse large B-cell lymphoma (DLBCL), respectively (2). Targeting of the B-cell receptor (BCR) pathway through inhibition of Bruton tyrosine kinase (BTK) with the first-in-class irreversible inhibitor ibrutinib has demonstrated exceptional clinical activity as a monotherapy for various subtypes of B-NHL, most notably CLL (3) and mantle cell lymphoma (MCL; ref. 4), but also Waldenström macroglobulinemia (WM; ref. 5) and activated B-cell-like DLBCL (ABC-DLBCL; ref. 6). Nonetheless, resistance to ibrutinib has been observed due in part to the acquisition of mutations that either affect the irreversible binding of BTK inhibitors (BTKi) or activate the phospholipase C gamma 2 (PLCγ2) enzyme, a downstream enzyme in the BTK pathway (7). In the case of BTK, a cysteine-to-serine mutation (BTK^{C481S}) abrogates the covalent binding of ibrutinib to BTK and has been detected in up to 86% of relapsing patients with CLL, but only anecdotally in MCL relapsing patients (7–9). Additional intrinsic mechanisms of resistance involve activation of the noncanonical Nuclear factor κB (NF-κB)-inducible kinase (NIK)-NF-κB signaling in MCL (10, 11).

The use of distinct next-generation sequencing (NGS)-based genomic techniques including whole exome and targeted deep sequencing have been instrumental in identifying BTK^{C481S} mutation as a genetic cause of BTKi resistance (12, 13). More recently, global drug profiling using MS-based phosphoproteomics has been successfully employed to characterize drug mechanisms of action in single-agent therapy or

[1]Lymphoma Translational Group, Josep Carreras Leukaemia Research Institute, Badalona, Spain. [2]Laboratory of Immunopharmacology and Molecular Biology, Sao Francisco University Medical School, Braganca Paulista, São Paulo, Brazil. [3]Stem Cell Biology, Developmental Leukemia and Immunotherapy Group, Josep Carreras Leukaemia Research Institute, Badalona, Spain. [4]Department of Biomedicine, School of Medicine, University of Barcelona, Barcelona, Spain. [5]Centro de Investigación Biomédica en Red de Cáncer (CIBERONC), Instituto de Salud Carlos III, Barcelona, Spain. [6]Autonomous University of Barcelona, Barcelona, Spain. [7]Proteomics Unit, Josep Carreras Leukaemia Research Institute, Badalona, Spain. [8]Cancer Epigenetics Group, Josep Carreras Leukaemia Research Institute, Badalona, Spain. [9]Department of Pathology, Hospital Universitari General de Catalunya-Grupo Quironsalud, Sant Cugat del Vallès, Spain. [10]TG Therapeutics, New York, New York. [11]Institució Catalana de Recerca i Estudis Avançats (ICREA), Barcelona, Spain. [12]Department of Hematology, Vall d'Hebron University Hospital, Barcelona, Spain. [13]Experimental Hematology, Vall d'Hebron Institute of Oncology, Barcelona, Spain.

Note: Supplementary data for this article are available at Clinical Cancer Research Online (http://clincancerres.aacrjournals.org/).

E. Normant and G. Roué contributed equally as the co-senior authors of this article.

Corresponding Authors: Gaël Roué, Lymphoma Translational Group, Josep Carreras Leukaemia Research Institute, Badalona, 08916, Spain. E-mail: groue@carrerasresearch.org; and Emmanuel Normant, VP Preclinical Sciences, TG Therapeutics, 2 Gansevoort Street, New York, NY 10014. E-mail: enormant@tgtxinc.com

Clin Cancer Res 2021;27:6591–601

doi: 10.1158/1078-0432.CCR-21-1067

Translational Relevance

Covalent Bruton tyrosine kinase inhibitors (BTKi) have transformed the treatment of B-cell non–Hodgkin lymphoma (B-NHL), but their activities have been limited by off-target toxicity and acquired resistance. TG-1701 is a novel irreversible and highly specific BTKi currently under study in relapsed/refractory patients. Here we show that TG-1701 exerts similar activity than the first-in-class BTKi ibrutinib, although with greater selectivity, in *in vitro* and *in vivo* models of B-NHL. We also report for the first time that a phosphoproteomic-based approach can discriminate between TG-1701 early-responder and TG-1701 late-responder patients with B-NHL. Furthermore, the coupling of proteomic profiling and transcriptomic analysis allowed the identification of Ikaros signaling disruption as an event commonly found in early-responder patients, and a crucial determinant of TG-1701 efficacy in BTKi-sensitive and BTKi-resistant B-NHL cell lines and mouse xenografts.

multidrug combinations in solid cancers (14). In addition, a recent publication also showed that phosphoproteomic profiling can help to understand the role of BTKi in patients with CLL. In this study, CLL cells from patients with an unmutated immunoglobulin heavy chain gene (*IGVH*) status showed higher basal phosphorylation than patients with *IGVH*-mutated status (15).

Here, we present TG-1701, a novel, orally available, irreversible BTKi that exhibits improved selectivity when compared with ibrutinib (16), and shows activity in various models of B-NHL. A MS-based phosphoproteomic platform used to interrogate the effects of TG-1701 on patients with CLL enrolled in the phase I dose-escalation study (NCT03671590; refs. 17–19) pointed to the transcription factor Ikaros as both a potential biomarker of clinical activity and an important node downstream of BTK in the BCR pathway.

Materials and Methods

Patients

Blood samples were obtained from 6 patients with CLL treated on the NCT03671590 clinical trial (**Table 1**). Briefly, patients with relapsed or refractory histologically confirmed B-cell lymphoma or CLL were eligible and treated with TG-1701 orally once daily until disease progression or the occurrence of intolerable side effects. Patients received either 200, 300, or 400 mg TG-1701 daily (**Table 1**). On the first day of treatment, white blood cells were counted, the absolute lymphocyte count (ALC) calculated, and the normal lowest and normal highest ALC established (Supplementary Table S1). The percentage of CLL cells in each sample was the ratio of ALC subtracted from highest normal ALC and divided by total ALC. All patients provided written informed consent. Institutional Review Board approvals for the study protocol, amendments, and informed consent documents were obtained prior to study initiation; study procedures were conducted in accordance with the Declaration of Helsinki.

Cell lines

Seven MCL (REC-1$^{GFP+LUC+}$, JEKO-1, UPN-1, UPN-IbruR, GRANTA-519, Z-138, and MINO), two ABC-DLBCL (OCI-LY3 and HBL-1), and two follicular lymphoma (DoHH2 and RL) cell lines were cultured as described elsewhere (20, 21). JEKO-1, MINO, and REC-1 parental cells were obtained from ATCC cell bank (LGC Standards). DoHH-2, GRANTA-519, and RL cell lines were purchased at DSMZ. UPN-1 and Z-138 cells were provided by Dr. B. Sola (University of Caen). HBL-1 was provided by Dr. E. Valls (IDIBAPS). OCI-Ly3 was kindly provided by Dr. A. Staiger (Dr. Margarete Fischer-Bosch Institute of Clinical Pharmacology). Cell-line authentication was performed upon reception by short tandem repeat (STR) profiling, using AmpFlSTR Identifier Kit (Thermo Fisher Scientific), and based on available STR profiles. This analysis was then repeated every 6 months and up to 4 months prior to the submission of the present manuscript. Mycoplasm infection was routinely tested by PCR.

Drugs

TG-1701 was provided by TG Therapeutics, Inc. Ibrutinib was purchased from Selleckchem.

Xenograft mouse model and IHC staining

The MINO MCL xenograft model was generated by inoculating subcutaneously 6- to 7-week-old nude mice (Shanghai Ling Chang Experimental Animal Co., Ltd.) with 5×10^6 MINO cells. When tumor volume reached 100 to 200 mm^3, animals were randomized into five groups of 8 to10 mice each, and were dosed orally with TG-1701 (25, 50, or 100 mg/kg, orally, twice a day), ibrutinib (100 mg/kg, orally, twice a day), or vehicle for 21 days. The tumor volume (V) was calculated as: $V = 1/2 \times a \times b^2$, where a and b represent the length and width, respectively. In REC-1 and UPN-IbruR xenografts, CB17-SCID mice (Janvier labs) were inoculated subcutaneously with 10^7 REC-1$^{GFP+Luc+}$ cells or UPN-IbruR cells and monitored for tumor growth, bioluminescence signal, and vital parameters as described previously (21), in compliance with the Animal Ethics Committee of the autonomous University of Barcelona (registry number 38/18). Tumor-bearing mice received either TG-1701 (25 mg/kg, every day) or ibrutinib (25 mg/kg, every day) for 17 days. Tumor samples were snap-frozen in OCT medium (Sakura Tissue Tek) or formalin-fixed and paraffin-embedded prior to immunohistochemical (IHC) staining with primary antibodies against Ikaros (Cell Signaling Technology) and CD20 (Beckman Coulter). Preparations were evaluated using an Olympus microscope and MicroManager software.

Western blot analysis

Total and nuclear protein extracts were obtained from MCL cell lines and tumor specimens using RIPA (Sigma-Aldrich), the Nuclear/Cytosol Fractionation Kit (BioVision), and T-PER (Thermo Fisher Scientific) buffers, respectively, and subjected to SDS-PAGE, as described previously (22, 23). Membrane-transferred proteins were revealed by incubating with primary and secondary antibodies (Supplementary Materials and Methods) followed by chemiluminescence detection using the ECL system (Pierce) and a Fusion FX imaging system (Vilber Lourmat). Band intensity was quantified using Image J software and normalized to housekeeping protein (GAPDH or TUBULIN). Values were referred to the indicated control (i.e., predose sample or DMSO-treated cells) and added below the corresponding band. If not otherwise specified, representative data from $n = 2$ experiments are shown.

Proteomic and phosphoproteomic profiling

Peripheral blood mononuclear cells (PBMC) were obtained from a total of 6 patients with CLL before and after 4-hour treatment with TG-1701 (**Table 1**), using standard Ficoll-Hypaque density gradient. Proteins were extracted using a Urea-based buffer (6 M Urea, 100 mmol/L Tris-HCl pH 7.5) on a Bioruptor sonicator, followed by standard Lys-C and trypsin-mediated digestion. Proteomic quantitative analyses were performed using 13 of the 16 channels of a 16plex - Tandem Mass Tag (TMT) system, according to

Table 1. Clinical and biological characteristics of patients with CLL.

Patient	Age	Gender	Cytogenetic alterations	IGVH status	TG-1701 daily dose (mg)	Clinical outcome (% reduction)	% CLL cells
AII-0011	61	F	Trisomy 12	UM	400–300	PR (87%)	16
AIJ-0015	64	M	11q del, trisomy 12	M	400	PR (86%)	62
AIJ-0001	57	M	17p del, trisomy 12	M	200	SD (38%)	74
AIJ-0005	60	F	—	M	300	SD-PR (56%)	93
AII-0006	83	M	17p del, trisomy 12	UM	200	PR (66%)	98
AIK-0003	80	M	17p del	M	200	SD (lymphocytosis)	80

Abbreviations: PR, partial response; SD, stable disease.

manufacturer's instructions (Thermo Fisher Scientific). A small part of the sample (260 μg) was used for total proteome analysis, and remaining proteins were subjected to phosphoproteome enrichment using the High-Select TiO2 Phosphopeptide Enrichment Kit (Thermo Fisher Scientific). Total proteome and phosphopeptide fractions were fractionated in 24 and 9 fractions using a Zorbax Extent-C18 and the High pH Reversed-Phase Peptide Fractionation Kit (Thermo Fisher Scientific), respectively, with prior analysis on an Orbitrap Fusion Lumos Tribrid mass spectrometer. REC-1 and REC-BTK^{C481S} protein extracts were labeled in triplicates with two TMT10plex, using a single channel (131N) to label a pool of all the samples. TMT fractionation and MS analysis were performed as above. Raw data were processed in MaxQuant (RRID:SCR_014485) and analyzed as described in Supplementary Materials and Methods. Data have been deposited to the ProteomeXchange Consortium (http://proteomecentral.proteomexchange.org) via the PRIDE partner repository (PXD023231; ref. 24).

RNA sequencing (RNA-seq) analysis and real-time qPCR

Total RNA was extracted using TRizol (Thermo Fisher Scientific) following manufacturer's instructions and poly-A-tailed enriched mRNA selected. Paired-end stranded RNA libraries with 51 read-inward facing paired mates were prepared, following sequencing with Illumina's NovaSeq6000 at the Centro Nacional de Analisis Genomico (CNAG). Data analysis was performed as described in Supplementary Materials and Methods.

The reverse transcription reaction was performed using a High-Capacity cDNA Reverse Transcription Kit (Applied Biosystems). The mRNA expression was analyzed in triplicate by quantitative real-time PCR. Amplification was performed using SYBR Green-based detection (GoTaqPCR Master Mix; Promega). The relative expression of each gene was quantified by the comparative cycle threshold method (ΔΔCt). β-Actin, GAPDH, and B2M were used as endogenous controls.

Immunofluorescence

BTKi-treated REC-1 and JEKO-1 cells (2–3 × 10^5) were seeded on poly-L-lysine-coated glass coverslips and stained as previously (23) with anti-Ikaros antibody (Cell Signaling Technology). Fluorescence signal was acquired on a Leica microscope and quantified using the LAS X (Leica) and Image J (RRID:SCR_003070) softwares.

Generation of BTK^{C481S} and BTK^{KO} cell lines

CRISPR-Cas9 gene editing tool were used to generate REC-BTK^{C481S} and REC-BTK^{KO} cells. Briefly, REC-1$^{GFP+LUC+}$ cells were electroporated with SpCas9 nuclease and BTK-specific gRNA using a Neon Transfection System (Thermo Fisher Scientific). After 30 days, single clones obtained by limit dilution were checked for BTK protein levels and analyzed by Sanger sequencing. Complete gene edition protocol can be found in Supplementary Data.

Statistical analysis

Presented data are the means ± Standard Deviation or SEM of three independent experiments. All statistical analyses were done by using GraphPad Prism 4.0 software (RRID:SCR_002798). Comparison between two groups of samples was evaluated by nonparametric Mann–Whitney test to determine how response is affected by two factors. Pearson test was used to assess statistical significance of correlation. Results were considered statistically significant when P value < 0.05.

Results

TG-1701 is a novel irreversible BTK inhibitor, more selective than ibrutinib

In a binding assay on a panel of 441 human kinases, TG-1701 was more selective than ibrutinib, with a comparable BTK Kd (3 nmol/L vs. 1.5 nmol/L, respectively) and a lower binding to EGFR, ITK, TXK, and JAK3 (Kd 135-, >48-, 68-, and >94-fold higher than those of ibrutinib, respectively; **Fig. 1A** and Supplementary Table S2). A BTK kinase activity assay revealed a TG-1701 EC_{50} of 6.70 nmol/L, slightly higher than ibrutinib IC_{50} (1.65 nmol/L; **Fig. 1B** and Supplementary Table S3). Accordingly, in an *in vitro* BTK occupancy assay, TG-1701 and ibrutinib showed a similar dose-dependent capacity to displace a BTK-specific fluorescent probe in the BTKi-sensitive follicular lymphoma cell line DoHH-2 (20), with complete BTK occupancy at 30 and 10 nmol/L, respectively (**Fig. 1C**). Consistently, BCR downstream signaling was impaired in a concentration-dependent manner in IgM-stimulated cells, with maximal effects observed at 100 nmol/L for TG-1701 and 10 nmol/L for ibrutinib (**Fig. 1D**). These effects were associated with a mean TG-1701 GI_{50} of 6.4 μmol/L at 72 hours, in a set of 10 parental B-NHL cell lines, which was slightly inferior to mean ibrutinib GI_{50} (14.1 μmol/L), especially in MCL cell lines (4.3 μmol/L vs. 10.8 μmol/L, respectively; Supplementary Table S3). Given that the activity of both BTK inhibitors in MINO cells was similar to these mean values, the tumor growth inhibition (TGI) of TG-1701 was evaluated *in vivo* in the corresponding xenograft model. A 16-day treatment of mice bearing MINO-derived tumors with 25, 50, and 100 mg/kg TG-1701 achieved a 56%, 72%, and 78% TGI, respectively, comparable with the 70% TGI observed in the ibrutinib (100 mg/kg) arm (**Fig. 1E**). A single oral gavage with 50 mg/kg TG-1701 further confirmed a rapid dephosphorylation of BTK and AKT as early as 2 and 4 hours, respectively, which was maintained for at least 24 hours due to the irreversible nature of TG-1701–mediated BTK inhibition (**Fig. 1F**).

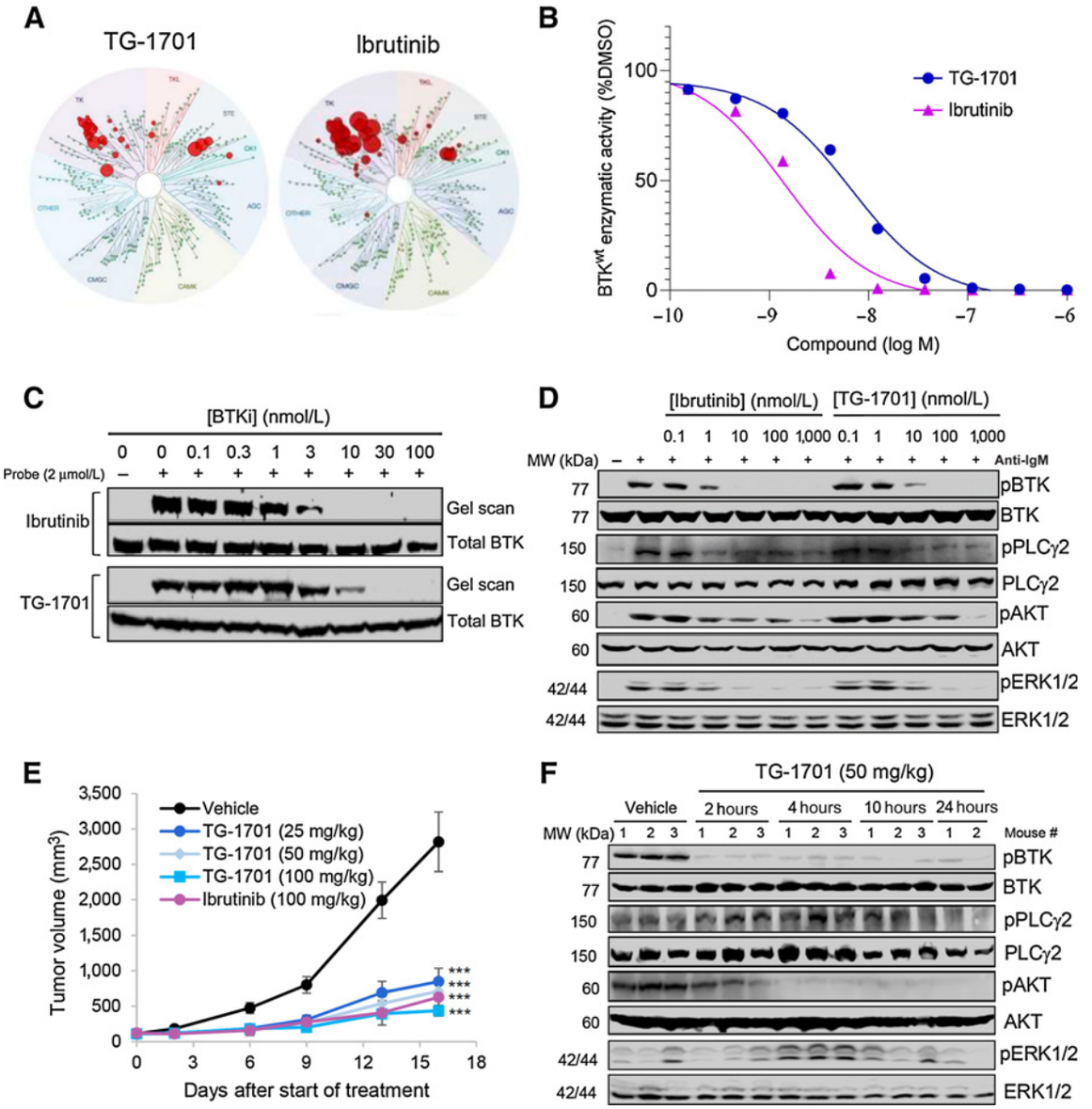

Figure 1.

TG-1701 is a novel irreversible BTK inhibitor as active as ibrutinib in *in vitro* and *in vivo* models of B-NHL. **A,** Binding of TG-1701 and ibrutinib 1 µmol/L was tested in a panel of 441 kinases using the DiscoverX technology. The size of each red circle is proportional to the strength of the binding. **B,** TG-1701 and ibrutinib BTK^{wt} anti-kinase activities were tested using a ^{33}P-ATP filtration assay. Shown are the average of two measurements. **C,** DoHH2 BTK-expressing cells were incubated with ibrutinib or TG-1701, lysed, and lysates were incubated with a fluorescent ibrutinib probe. Total BTK was assessed by Western blot analysis. **D,** Increasing concentrations of ibrutinib or TG-1701 were incubated with DoHH-2 cells for 20 minutes. BCR pathway was then activated with 10 µg/mL soluble goat F(ab')2 anti-IgM for 18 hours and levels of different downstream enzymes were assessed using Western blot analysis. **E,** TG-1701 or ibrutinib were dosed orally in the MINO MCL xenograft model and (**F**) intratumor levels of several BCR-related kinases were assessed by Western blot analysis.

Phosphoproteomic analysis differentiates early clinical outcomes and points to the inhibition of the Ikaros pathway as an important mechanism of TG-1701 activity

To identify potential biomarkers of TG-1701 activity in B-NHL, PBMCs from 6 patients with CLL enrolled in the TG-1701–101 phase I trial were isolated at different time points for omics analysis. In all patient samples but one, the percentage of circulating cancer cells was comprised between 60% and 98% (**Table 1**; Supplementary Table S1). All the patient samples harbored a wild-type BTK gene, as confirmed by Sanger sequencing of *BTK* exon 11 (data not shown).

Near-complete BTK occupancy was obtained in all samples tested (**Fig. 2A**) and linear kinetics was observed with approximately dose-proportional increases in C_{max} and $AUC_{0-8\ hours}$ from 100 to 300 mg (Supplementary Fig. S2; ref. 18), with a positive correlation between the daily dose and TG-1701 C_{max} for the

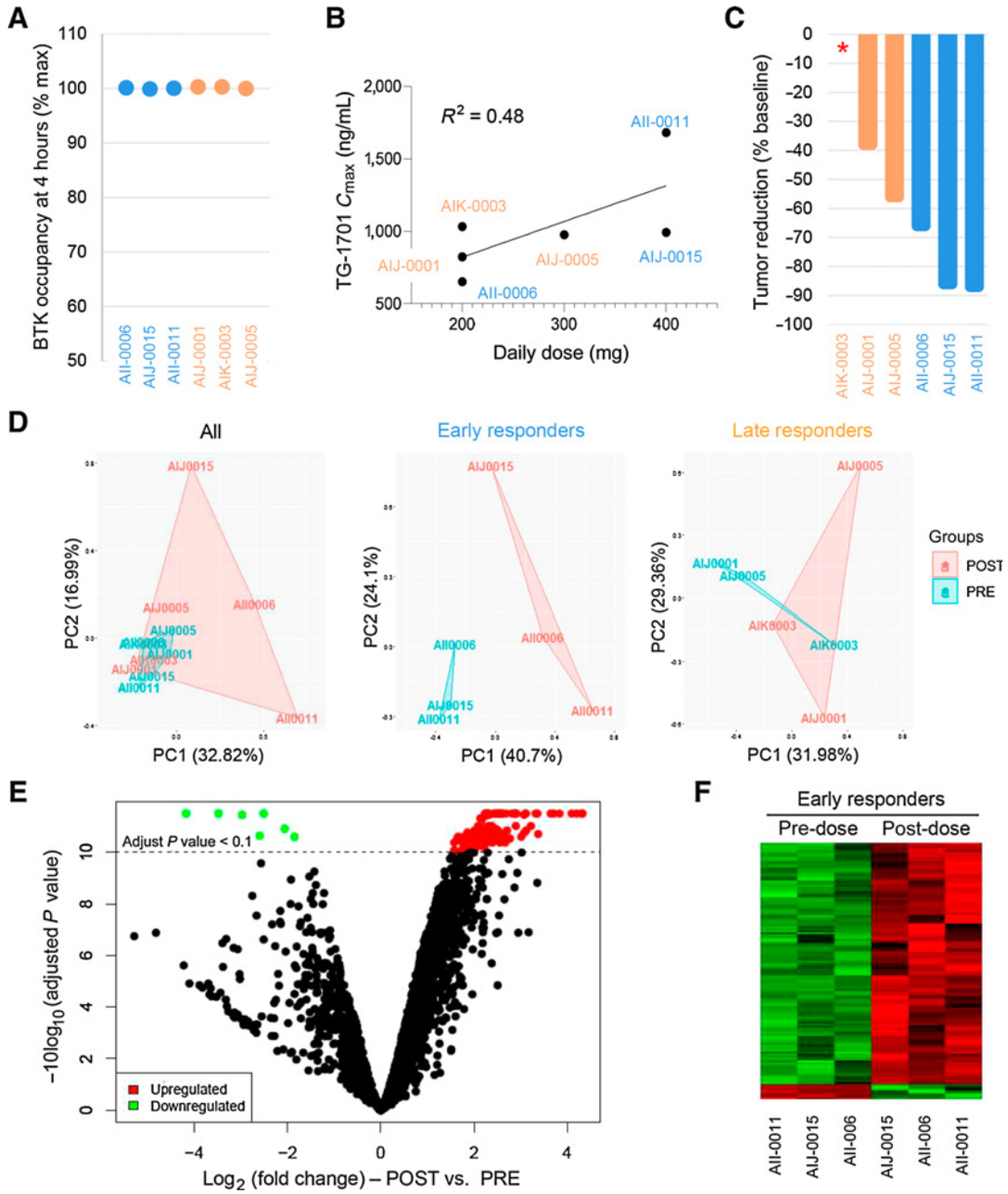

Figure 2.

Phosphoproteomic analysis of 6 patients with CLL treated with TG-1701 can segregate early and late responders. **A,** BTK occupancy was assessed in all patients in the study at nine different time points. Here the occupancy of the 6 patients with CLL are shown at 4 hours after treatment. The occupancy assay was run using a MSD method (as depicted in Supplementary Fig. S1) at Bioagilytix. **B,** Correlation of TG-1701 C_{max} and the daily dose received by the 6 patients. **C,** Best tumor reduction in all 6 patients at C3D1. *AIK-003 lymphocytosis at C3D1 rank the response as a stable disease. **D,** Phosphoproteomic profiling and principal components analysis were performed on all 6 patients with CLL (left), 3 early responders (middle), and 3 late responders (right). Pretreatment samples are shown in blue and the 4-hour posttreatment samples in red. Percentages refer to the total variance explained for each component. **E,** Quantified phosphopeptides in early responders. Volcano plot of the early responders–only samples. The late responders do not exhibit any TG-1701–driven changes. **F,** The phosphosites that are up- or downregulated are shown for 3 single patients.

6 patients studied (**Fig. 2B**). After three cycles of treatment, the best change in tumor burden as assessed by CT scan ranged from 38% to 87%, with 1 tumor-free patient with a lymphocytosis that defined his best response as a stable disease (**Fig. 2C**).

In PBMC protein extracts from the six predose and the six 4-hour postdose samples, a total of 5,585 proteins and 2,438 phosphosites were identified. An initial principal component analysis (PCA) did not discriminate the pretreatment (PRE) from the posttreatment (POST)

profiles. However, a specific unsupervised clustering of the data into two subgroups of 3 patients allowed a clear differentiation between the PRE and POST samples (**Fig. 2D**). These two subgroups, blindly selected to uncover changes due to TG-1701 treatment, clearly fitted the clinical outcome of the patients (**Fig. 2C**), separating *de facto* a group encompassing the 3 best responses (called the early responders) and a group gathering the 3 other patients with lower responses (called the late responders). Supporting this partition of the patients, the early responders exhibited a stronger *IL10* de-repression and a stronger, although not significant, decrease in *IL2* and *IL6* expression (Supplementary Fig. S3A), suggesting that they developed a more potent early anti-inflammatory response, a common feature of BTKi activity (25). In addition, *CCL3* and *CCL4* chemokine genes, two *bona fide* biomarkers for BCR pathway activation (26), were more downregulated in early-responder patients (Supplementary Fig. S3A). A set of 118 phosphopeptides were differentially phosphorylated (7 down- and 111 upregulated) after TG-1701 treatment in the early-responder subgroup only (adjusted P value < 0.1; **Fig. 2E**). These sites corresponded to the putative modulation of 14 protein kinases (Supplementary Tables S4 and S5). Importantly, these quantitative phosphoproteomic changes showed a strong homogeneity in the 3 early-responder patients and enabled a clear distinction between PRE and POST samples (**Fig. 2F**). Only one single phosphosite (UBA1-pSer4) was found significantly upregulated in the late-responder patients after TG-1701 treatment.

Beside the 118 phosphosites mentioned above and depicted in **Fig. 2E**, another set of 96 phosphopeptides were present in pretreatment samples and totally dephosphorylated upon treatment with TG-1701. The total absence of phosphorylation preempted the statistical analysis and incorporation of these 96 samples in the volcano plot, even though these sites were the most impacted by TG-1701 treatment. Of special interest, the corresponding list of phosphosites comprised the p-Ser442/445 residue of Ikaros, a zinc finger-containing DNA-binding protein that plays a pivotal role in B-cell homeostasis. Ikaros-Ser442/445 dephosphorylation was indeed the strongest event associated with TG-1701 activity (Supplementary Table S6). Because Ikaros nuclear localization and transcriptional activity both depend on BTK-mediated phosphorylation at Ser214/215 residues (27), we investigated whether, analogously, Ikaros function was differentially affected by TG-1701 in early-responder versus late-responder CLL patient samples. Using previously validated Ikaros-repressed and Ikaros-enhanced gene signatures (28), we identified 21 proteins of the repressed signature that were upregulated, whereas another set of 17 factors from the Ikaros-enhanced gene signature were depleted only in early responders, suggesting that Ikaros was functionally impaired after TG-1701 treatment (**Fig. 3A**). Although a comparative multidimensional (MDS) analysis of RNA-seq data obtained from the same subset of samples failed to show a clear difference between early-responsive and late-responsive patient clusters (Supplementary Fig. S3B), a clear trend in the upregulation of Ikaros-repressed genes and downregulation of Ikaros-enhanced genes was seen in TG-1701 early-responsive patients only (**Fig. 3B**). Accordingly, the IKZF1-repressed gene, *YES1*, was significantly upregulated, whereas the IKZF1-enhanced gene *MYC* was downregulated in early responders but not in late responders (**Fig. 3C**). Importantly, this effect was not due to Ikaros protein destabilization, as its level of expression did not vary upon TG-1701 treatment in early-responder patients, whereas the expression of p-BTK and MYC proteins underwent a 70% and 48% downregulation, respectively, and the levels of YES1 increased by almost 5-fold (**Fig. 3D**; Supplementary Fig. S3C). Such modifications were not seen in late-responder patients, although BTK was notably dephosphorylated (**Fig. 3D**; Supplementary Fig. S3C). These data were confirmed *in vitro* using the ibrutinib-sensitive MCL cell line REC-1 characterized by ibrutinib and TG-1701 GI_{50} values of 5.82 and 3.83 μmol/L at 72 hours, respectively (Supplementary Table S3). In these cells, as observed in early-responder patients with CLL, TG-1701 treatment led to efficient BTK dephosphorylation, *YES1* upregulation, and *MYC* downregulation both at mRNA and protein levels (**Fig. 3E** and **F**). Of note, among the *IKZF1*-target genes studied here, *YES1* reactivation was significantly higher in TG-1701–treated than in ibrutinib-exposed cells (**Fig. 3E**). Finally, **Fig. 3G** shows that ibrutinib and TG-1701 elicited a 67% to 83% and a 80% to 85% reduction in nuclear Ikaros, consistent with a nearly 50% to 70% decrease of Ikaros in REC-1 and JEKO-1 nuclear protein fraction (**Fig. 3H**), suggesting that dual dephosphorylation of Ikaros at Ser442 and Ser445 was associated with the nuclear exclusion of this factor.

Ikaros signature is a *bona fide* hallmark of BTKi mechanism of action

To further explore TG-1701 mechanisms of action and potential mechanisms of resistance, we CRISPR-engineered the REC-$1^{GFP+LUC+}$ cell line to express the BTK^{C481S}. This mutation was associated with a 10.3- and a 54.8-fold decrease in ibrutinib and TG-1701 inhibitory kinase activity, respectively (Supplementary Fig. S4A; Supplementary Table S3). The REC-1–BTK^{C481S} cell line was 4.2- and 2.8-fold less sensitive to ibrutinib and TG-1701 respectively, compared with parental REC-1 cells (**Fig. 4A**; Supplementary Table S3). A washout experiment further showed that irreversible BTK inhibition—illustrated by kinase phosphorylation over 24 hours after BTKi removal in REC-1 cells—was mostly lost in REC-1–BTK^{C481S} cells (**Fig. 4B**). Although total proteome composition was modified solely in the parental cells treated with either ibrutinib or TG-1701 as assessed by PCA analysis (Supplementary Fig. S4B), a set of 16 Ikaros-repressed proteins were upregulated and another set of 14 Ikaros-upregulated proteins were downregulated in REC-1, but not in REC-1–BTK^{C481S} cells exposed to TG-1701 (**Fig. 4C**). Despite the short drug exposure, transcriptional upregulation of *YES1*, and repression of *MYC* were observed in BTK^{wt} cells treated with both BTKis. In REC-1–BTK^{C481S} cells, a pronounced basal Ikaros-repressed gene signature was observed in the absence of any treatment (black bars, **Fig. 4D**), including *YES1* expression, and this pattern was not modified upon BTKi exposure (**Fig. 4D**; Supplementary Fig. S4C).

To confirm the role of BTK as an upstream regulator of Ikaros signaling in BTKi-exposed cells, we generated a BTK knockout (KO) model derived from the REC-1 cell line, using a CRISPR-Cas9 method, as described above. The obtained REC-BTK^{KO} derivative, characterized by an almost complete depletion of BTK (**Fig. 4E**) was refractory to both ibrutinib and TG-1701 (Supplementary Table S3) and did not undergo significant modulation of *YES1* and *MYC* expression after exposure to TG-1701 (**Fig. 4E** and **F**). To validate the relevance of the BTK-Ikaros signaling axis in the regulation of YES1 and MYC upon BTK inhibition, two CRISPR-Cas9–engineered cell lines either devoid of Ikaros (REC-$IKZF1^{KO}$) or with *de novo* expression of BTK after BTK gene knockout (REC-$BTK^{KO\text{-}OE}$) were generated (see Supplementary Materials and Methods). Supplementary Figure S5A and S5B shows that Ikaros depletion was accompanied by a 2- to 3-fold increase in YES1 expression in REC-1 cells, and that no further upregulation of this gene could be achieved after BTK inhibition. MYC expression did not undergo significant variation upon treatment with either TG-1701 or ibrutinib. Most interestingly, the re-introduction of an IgM-responsive form of BTK within REC-BTK^{KO} cells, restored the capacity of TG-1701, and in a lesser extent ibrutinib, to suppress the Ikaros-

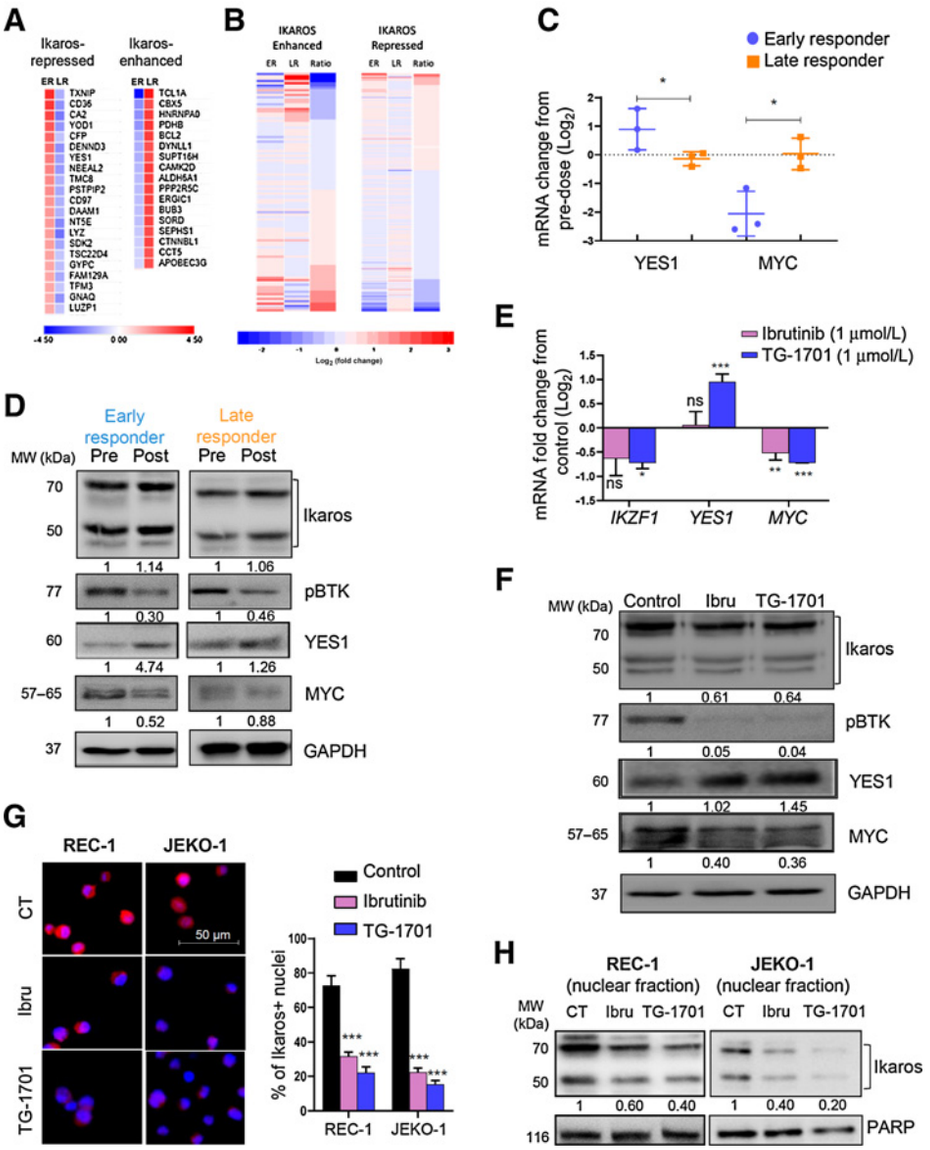

Figure 3.

Impairment of Ikaros signaling is associated with B-NHL response to TG-1701 in both clinical and preclinical settings. Change of Ikaros-regulated factors upon TG-1701 treatment in early responders (ER) and late responders (LR), according to (**A**) total proteome data and (**B**) RNA-seq analysis of the same samples. For each category, the average of the 3 patients is displayed. **C,** *YES1* (an Ikaros-repressed gene) and *MYC* (an Ikaros-enhanced gene) mRNA changes after TG-1701 treatment. **D,** Immunoblot evaluation of p-BTK, Ikaros, and Ikaros downstream factors, MYC and YES1, using one representative early- and one late-responder PBMC lysates. P-BTK detection was assessed to confirm on-target activity at 4 hours posttreatment. MCL REC-1 cells were treated for 24 hours with 1 μmol/L ibrutinib or TG-1701, and variations in Ikaros-regulated factors were quantified using (**E**) qPCR and (**F**) Western blot analysis. Subcellular localization of Ikaros was determined by (**G**) immunofluorescence staining (red signal, counterstained by DAPI nuclear labelling in blue) and (**H**) immunoblot analysis of nuclear protein fraction, in REC-1 and JEKO-1 cells treated as above with ibrutinib or TG-1701 (*, $P < 0.05$; **, $P < 0.01$; ***, $P < 0.001$; ns, nonsignificant).

dependent repression of YES1 and upregulation of MYC (Supplementary Fig. S5C and S5D). Altogether, these data strongly suggest that TG-1701–dependent impairment of Ikaros signaling in MCL cells is a BTK-dependent process.

Given the low recurrence of BTK^{C481S} mutation in patients with MCL (9), the UPN-IbruR noncanonical NF-κB–driven ibrutinib resistance model was also studied (20). This subclone is characterized by the absence of mutations in the *BTK* and *PLCG2* genes and the constitutive activation of p52-dependent signaling, driving a 2- to 3-fold increase in ibrutinib and TG-1701 GI_{50} at 72 hours (Supplementary Fig. S4D; Supplementary Table S3; ref. 20). When compared with the BTKi-sensitive REC-1 xenograft model in which a 17-day dosing with TG-1701 achieved a 53% tumor TGI versus vehicle, UPN-IbruR tumors were almost insensitive to TG-1701 (**Fig. 5A**). Accordingly, p-BTK was efficiently downregulated in representative REC-1 tumor specimens, but not in UPN-IbruR xenografts treated with TG-1701 (**Fig. 5B**). In agreement with *in vitro* results, MYC was downregulated, and YES1 upregulated at protein and/or mRNA levels, in association with Ikaros nuclear exclusion and a decrease in $CD20^{+}$ malignant B cells, in BTKi-sensitive, but not in BTK-insensitive MCL xenografts (**Fig. 5B–D**).

Discussion

During the past decade, BTK inhibitors have increasingly replaced chemotherapy-based regimens in patients with CLL and MCL. TG-1701 is a novel second-generation BTKi currently under clinical development. TG-1701 is more selective than ibrutinib, with a comparable BTK Kd and similar *in vitro* and *in vivo* characteristics. TG-1701 is currently being tested in a phase I trial comprised of a single-agent arm and a combination arm with ublituximab (a novel CD20 antibody) and umbralisib (a dual PI3Kδ and CKIε inhibitor). With a median follow-up of 7 months in a 200 mg daily monotherapy expansion cohort, preliminary overall response rates (ORR) are 95%

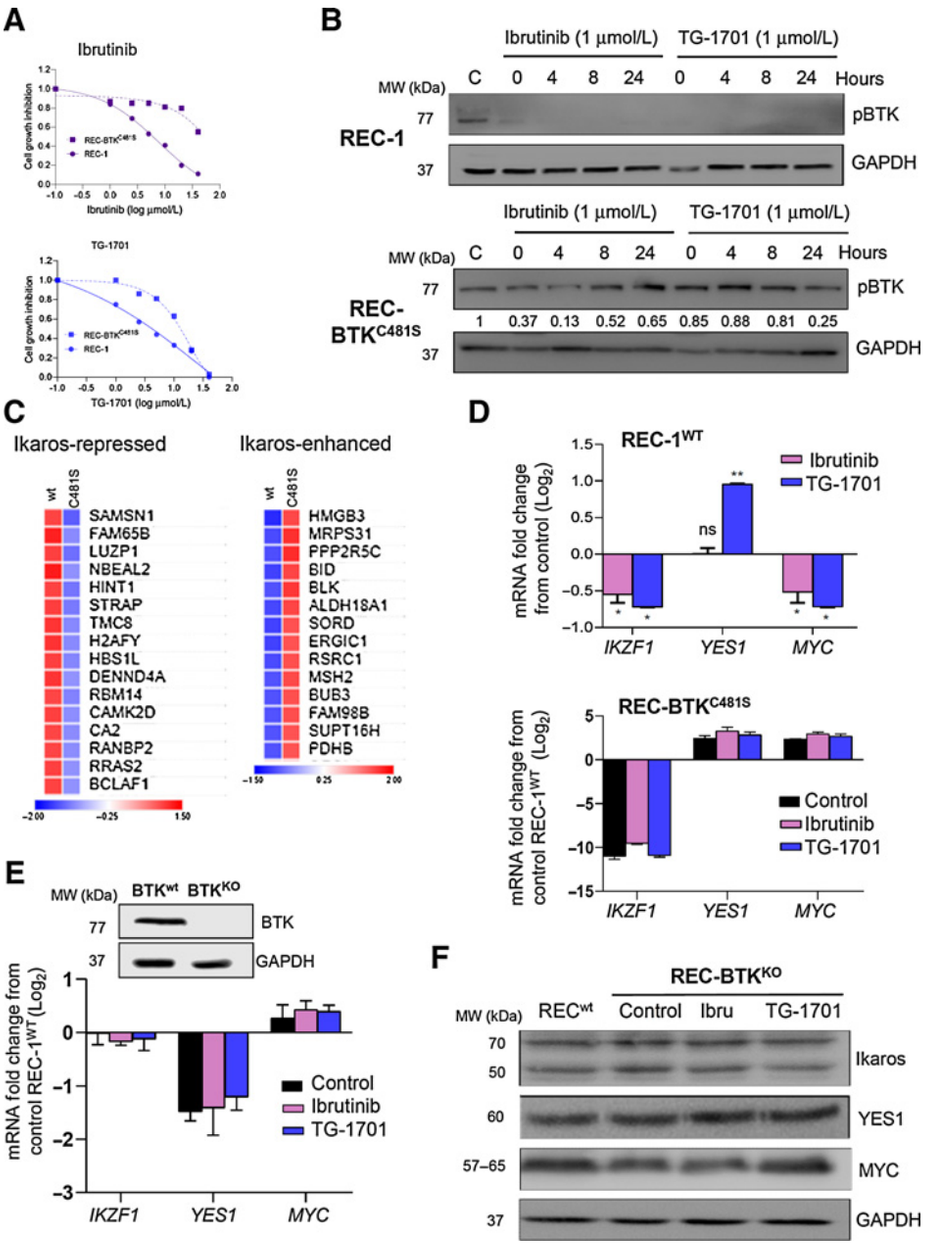

Figure 4.

Ikaros modulation is associated with TG-1701 efficacy in distinct *in vitro* and *in vivo* MCL models of ibrutinib resistance. **A,** Viability of BTK^{wt} and BTK^{C481S} REC-1 cells exposed to increasing doses of ibrutinib and TG-1701 was evaluated by CellTiter Glo assay. **B,** REC-1 and REC-1–BTK^{C481S} cells were exposed for 1 hour to 1 µmol/L TG-1701, washed-out for the indicated times, and levels of phospho- and total BTK were assessed using immunoblotting. Values below immunoblot correspond to the densitometric quantification of p-BTK/GADPH ratio. **C,** Regulation of Ikaros-regulated factors after 4 hours of treatment with TG-1701 or ibrutinib (1 µmol/L) in REC-1 and REC-1–BTK^{C481S} cells according to total proteome data. **D,** Ikaros gene signatures were evaluated by qPCR in REC-1 and REC-1–BTK^{C481S} cells exposed for 24 hours to 1 µmol/L ibrutinib or TG-1701. In REC-1–BTK^{C481S} cells, values were referred to untreated REC-1 cells (control). Ikaros transcriptional (**E**) and protein (**F**) signatures were evaluated in REC-1–BTK^{KO} cells as previously, using untreated REC-1 cells as a reference control.

(19/20) in CLL, 50% (9/18) in MCL, and 95% (18/19) in WM. No complete responses (CR) are confirmed on TG-1701 monotherapy (17). In this study, we show that phosphoproteomic analysis of pre- and posttreatment samples clustered patients with CLL according to their early clinical responses (early responders vs. late responders) and helped decipher the mechanisms underlying drug responsiveness. According to the results, the response from these patients did not depend on the pharmacokinetic or pharmacodynamic properties of TG-1701, but rather on differences in BTK downstream signaling. In early-responder patients, Ikaros-p-Ser442/445 was the phosphopeptide most impacted (dephosphorylated) by TG-1701 treatment and several Ikaros-dependent factors were transcriptionally deregulated, suggesting that Ikaros may represent a biomarker for early response, and/or an important new node downstream BTK inhibition. Interestingly, a recent study in acalabrutinib-treated patients with CLL (15) has shown that the unmutated *IGVH* cells displayed a higher basal phosphorylation level compared with the mutated *IGVH* cells, showing that the phosphoproteomic profile of BTKi-treated patients can cluster specific subgroups of patients.

Ikaros is a zinc finger protein involved in gene regulation and chromatin remodeling. Its nuclear localization, stability, and transcriptional activity depend on its phosphorylation status, which is regulated by BTK, casein kinase II (CKII), and protein phosphatase 1 (PP1) interplay (27, 29). Although the exact role of serine residues at position 442 and 445 is still unknown, their juxtaposition to the conserved PP1 binding motif in the C-terminal end of Ikaros protein (30) might confer them a role in the PP1-mediated regulation of Ikaros stability and pericentromeric localization (29).

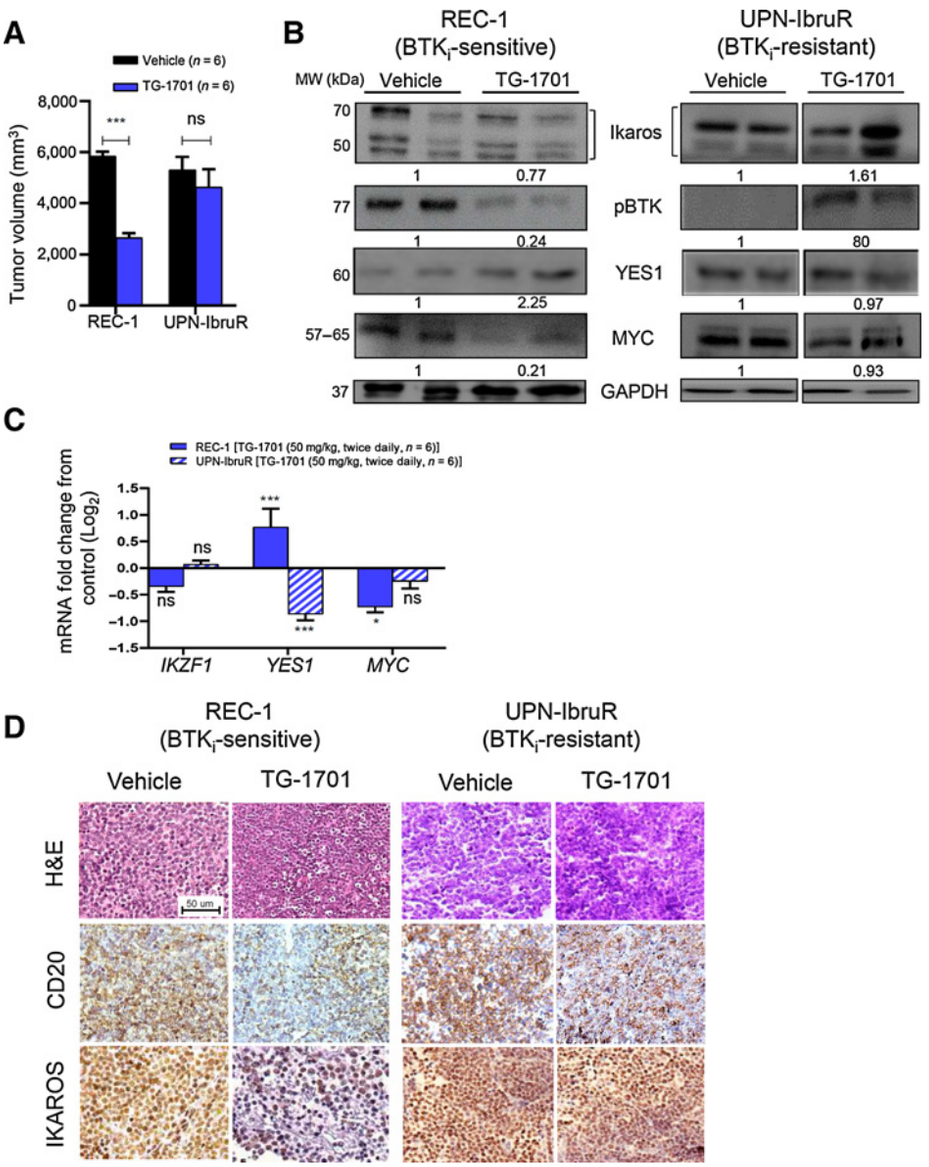

Figure 5.

In vivo activity of TG-1701 on BTKi-sensitive and BTKi-resistant MCL mouse models. **A,** TG-1701 was dosed orally in BKT_i-sensitive (REC-$1^{GFP+LUC+}$) and BTK_i-resistant (UPN-IbruR) MCL xenograft models and tumor volumes were recorded at the endpoint (17 days) by bioluminescence signal recording (REC-1) or external calipers (UPN-IbruR). Ikaros signature was evaluated by (**B**) Western blot analysis and (**C**) qPCR in 2/3 representative tumors from each treatment group. Densitometric quantification of Ikaros, phospho-BTK, and MYC protein levels were normalized to GAPDH levels and referred to vehicle-treated tumors. For each treatment group, the average of the two tumors is shown. **D,** IHC labeling of CD20 and Ikaros in tissue sections from four representative BTKi-sensitive (REC-1) and BTKi-resistant (UPN-IbruR) tumor specimens (scale bar: 25 µm; *, $P < 0.05$; **, $P < 0.01$; ***, $P < 0.001$; ns, nonsignificant).

Interestingly, CKII was ranked #4 in the list of kinases with reduced activity in TG-1701 early-responder patients, whereas phosphorylation of the PP1 inhibitory subunit, PPP1R14A, and dephosphorylation of the PP1 inhibitor, PPP1R2, both associated with reduced PP1 activity (31), were among the top four modifications detected in TG-1701 early-responder patients (Supplementary Tables S4 and S5). Ikaros expression was affected by TG-1701 treatment, neither in CLL primary cells nor in BTKi-sensitive REC-1 models, indicating that the inhibition of Ikaros signature in early responders was more likely due to a nuclear exclusion of the transcription factor. Importantly, our results obtained in REC-1–BTK^{C481S} and REC-1–BTK^{KO} subclones demonstrated that both the cell proliferation blockade and the modulation of Ikaros activity upon TG-1701 treatment are tightly dependent on the presence of a wild-type BTK protein, supporting the idea that Ikaros phosphorylation at Ser442/445 is controlled by the kinase, and discarding a potential off-target effect of the compound. Downregulation of the Ikaros program in BTK^{C481S} cell line is not understood at that point. One possible explanation is that the C481S mutation does not only abrogate the irreversibility of ibrutinib or TG-1701 binding but also modifies the substrate specificity of the newly formed substrate pocket that would not phosphorylate Ikaros anymore. Further studies involving the production of a phospho-specific Ikaros-Ser442/445 antibody will be required to confirm this hypothesis.

The number of samples tested in this study is too small to draw definitive conclusions, and because responses to BTKis continue to deepen over time (as long as 2 years), the early (C3D1) timepoint may not fully represent the overall drug efficacy. However, the differences presented here between "early-responders" and "late-responders" are clear enough to warrant future studies, for example testing an enlarged pool of patient samples treated with BTKis or exploring other NHLs. In addition, other (non-Ikaros) potential biomarkers for which an existing phospho-antibody is commercially available could be evaluated. In the study presented here, the assessment of the clinical

outcome available at the time of analysis was the first CT scan, after two cycles of treatment. Assessing the phosphorylation status of the biomarkers presented here in patients who progressed under, or become resistant to BTKi treatment, might also help understand the underlying mechanisms of activity or resistance.

Authors' Disclosures

H. Miskin reports personal fees from TG Therapeutics, Inc. during the conduct of the study. P. Menéndez reports personal fees from OneChain Immunotherapeutics outside the submitted work. E. Normant reports employment and ownership of stock with TG Therapeutics. G. Roué reports grants from TG Therapeutics and Instituto de Salud Carlos III during the conduct of the study. No disclosures were reported by the other authors.

Authors' Contributions

M.L. Ribeiro: Resources, investigation, methodology, writing–original draft. **D. Reyes-Garau:** Investigation, methodology. **M. Vinyoles:** Resources, validation, investigation, writing–review and editing. **N. Profitós Pelejà:** Investigation, methodology. **J.C. Santos:** Investigation, methodology. **M. Armengol:** Investigation. **M. Fernàndez-Serrano:** Investigation. **A. Sedó Mor:** Investigation, methodology. **J.J. Bech-Serra:** Data curation, software, visualization. **P. Blecua:** Data curation, software, visualization. **E. Musulen:** Investigation, methodology. **C. De La Torre:** Formal analysis, investigation, methodology. **H. Miskin:** Validation, writing–review and editing. **M. Esteller:** Data curation, writing–review and editing. **F. Bosch:** Writing–review and editing. **P. Menéndez:** Validation, investigation, methodology, writing–review and editing. **E. Normant:** Conceptualization, resources, supervision, validation, writing–original draft, writing–review and editing. **G. Roué:** Conceptualization, resources, supervision, funding acquisition, validation, investigation, visualization, writing–original draft, project administration, writing–review and editing.

Acknowledgments

We are very grateful to Dr. Chan Cheah at Linear Clinical Research, Dr. Constantine Tam at St. Vincents private hospital in Melbourne, and Dr. Nick Wickham at Adelaide Cancer Center in Ashford, as well as the TG Therapeutics clinical team led by Dr. Alejandro Ricart for their precious help. The authors would like to thank the CNAG-CRG for assistance with RNA sequencing. This study was financially supported by Fondo de Investigación Sanitaria PI18/01383, European Regional Development Fund (ERDF) "Una manera de hacer Europa" (to G. Roué), and TG Therapeutics. J.C. Santos and M. Fernández-Serrano were recipients of a Sara Borrell research contract (CD19/00228) and a predoctoral fellowship (FI19/00338) from Instituto de Salud Carlos III, respectively. M. Armengol was a fellow of PROTEOblood (EFA360/19), a project co-financed by the ERDF through the Interreg V-A Spain-France-Andorra (POCTEFA) program. This work was carried out under the CERCA Program (Generalitat de Catalunya).

The costs of publication of this article were defrayed in part by the payment of page charges. This article must therefore be hereby marked *advertisement* in accordance with 18 U.S.C. Section 1734 solely to indicate this fact.

Received March 24, 2021; revised July 7, 2021; accepted September 17, 2021; published first September 22, 2021.

References

1. Fisher SG, Fisher RI. The epidemiology of non-Hodgkin's lymphoma. Oncogene 2004;23:6524–34.
2. Quintanilla-Martinez L. The 2016 updated WHO classification of lymphoid neoplasias. Hematol Oncol 2017;35:37–45.
3. Byrd JC, Furman RR, Coutre SE, Flinn IW, Burger JA, Blum KA, et al. Targeting BTK with ibrutinib in relapsed chronic lymphocytic leukemia. N Engl J Med 2013;369:32–42.
4. Wang ML, Rule S, Martin P, Goy A, Auer R, Kahl BS, et al. Targeting BTK with ibrutinib in relapsed or refractory mantle-cell lymphoma. N Engl J Med 2013; 369:507–16.
5. Treon SP, Tripsas CK, Meid K, Warren D, Varma G, Green R, et al. Ibrutinib in previously treated Waldenström's macroglobulinemia. N Engl J Med 2015;372: 1430–40.
6. Wilson WH, Young RM, Schmitz R, Yang Y, Pittaluga S, Wright G, et al. Targeting B cell receptor signaling with ibrutinib in diffuse large B cell lymphoma. Nat Med 2015;21:922–6.
7. Woyach JA, Furman RR, Liu T-M, Ozer HG, Zapatka M, Ruppert AS, et al. Resistance mechanisms for the Bruton's tyrosine kinase inhibitor ibrutinib. N Engl J Med 2014;370:2286–94.
8. Furman RR, Cheng S, Lu P, Setty M, Perez AR, Guo A, et al. Ibrutinib resistance in chronic lymphocytic leukemia. N Engl J Med 2014;370:2352–4.
9. Chiron D, Di Liberto M, Martin P, Huang X, Sharman J, Blecua P, et al. Cell-cycle reprogramming for PI3K inhibition overrides a relapse-specific C481S BTK mutation revealed by longitudinal functional genomics in mantle cell lymphoma. Cancer Discov 2014;4:1022–35.
10. Wu J, Liu C, Tsui ST, Liu D. Second-generation inhibitors of Bruton tyrosine kinase. J Hematol Oncol 2016;9:80.
11. Rahal R, Frick M, Romero R, Korn JM, Kridel R, Chan FC, et al. Pharmacological and genomic profiling identifies NF-kappaB-targeted treatment strategies for mantle cell lymphoma. Nat Med 2013;20:87–92.
12. Doostparast Torshizi A, Wang K. Next-generation sequencing in drug development: target identification and genetically stratified clinical trials. Drug Discov 2018;23:1776–83.
13. Wacker SA, Houghtaling BR, Elemento O, Kapoor TM. Using transcriptome sequencing to identify mechanisms of drug action and resistance. Nat Chem Biol 2012;8:235–7.
14. Carvalho AS, Matthiesen R. Global MS-based proteomics drug profiling. Methods Mol Biol 2016;1449:469–79.
15. Beckmann L, Berg V, Dickhut C, Sun C, Merkel O, Bloehdorn J, et al. MARCKS affects cell motility and response to BTK inhibitors in CLL. Blood 2021;138: 544–56.
16. Normant E, Gorelik L, Shmeis R, Le H, Nisch R, Miskin HP, et al. TG-1701 a novel, orally available, and covalently-bound BTK inhibitor. EHA Library. 2018 [Internet]. [cited 2020 Oct 31]. Available from: https://library.ehaweb.org/eha/2018/stockholm/215080/emmanuel.normant.phd.tg-1701.a.novel.orally.available.and.covalentlybound.btk.html?f=listing%3D0%2Abrowseby%3D8%2Asortby%3D1%2Asearch%3Dtg-1701.
17. Cheah CY, Wickham N, Jurczak W, Lasica M, Wróbel T, Walewski J, et al. Clinical activity of TG-1701, as monotherapy and in combination with ublituximab and umbralisib (U2), in patients with B-cell malignancies [ASH abstract 1130]. Blood 2020;136(suppl 1).
18. Cheah CY, Wickham N, Yannakou CK, Lewis KL, Hui C-H, Tang PS, et al. Safety and activity of the once daily selective Bruton kinase (BTK) inhibitor TG-1701 in patients with chronic lymphocytic leukemia (CLL) and lymphoma. HemaSphere 2020;4:309.
19. Cheah CY, Wickham N, Yannakou CK, Lewis KL, Hui C-H, Tang PS, et al. Phase 1 study of TG-1701, a selective irreversible inhibitor of Bruton's tyrosine kinase (BTK), in patients with relapsed/refractory B-cell malignancies. Blood 2019;134:4001.
20. Balsas P, Esteve-Arenys A, Roldán J, Jiménez L, Rodríguez V, Valero JG, et al. Activity of the novel BCR kinase inhibitor IQS019 in preclinical models of B-cell non-Hodgkin lymphoma. J Hematol Oncol 2017;10:80.
21. Body S, Esteve-Arenys A, Miloudi H, Recasens-Zorzo C, Tchakarska G, Moros A, et al. Cytoplasmic cyclin D1 controls the migration and invasiveness of mantle lymphoma cells. Sci Rep 2017;7:13946.
22. Pérez-Galán P, Mora-Jensen H, Weniger MA, Shaffer AL, Rizzatti EG, Chapman CM, et al. Bortezomib resistance in mantle cell lymphoma is associated with plasmacytic differentiation. Blood 2011;117:542–52.
23. Esteve-Arenys A, Valero JG, Chamorro-Jorganes A, Gonzalez D, Rodriguez V, Dlouhy I, et al. The BET bromodomain inhibitor CPI203 overcomes resistance to ABT-199 (venetoclax) by downregulation of BFL-1/A1 in in vitro and in vivo models of MYC+/BCL2+ double hit lymphoma. Oncogene 2018;37:1830–44.

24. Perez-Riverol Y, Csordas A, Bai J, Bernal-Llinares M, Hewapathirana S, Kundu DJ, et al. The PRIDE database and related tools and resources in 2019: improving support for quantification data. Nucleic Acids Res 2019;47:D442–50.
25. Purvis GSD, Collino M, Aranda-Tavio H, Chiazza F, O'Riordan CE, Zeboudj L, et al. Inhibition of Bruton's TK regulates macrophage NF-κB and NLRP3 inflammasome activation in metabolic inflammation. Br J Pharmacol 2020; 177:4416–32.
26. Takahashi K, Sivina M, Hoellenriegel J, Oki Y, Hagemeister FB, Fayad L, et al. CCL3 and CCL4 are biomarkers for B cell receptor pathway activation and prognostic serum markers in diffuse large B cell lymphoma. Br J Haematol 2015; 171:726–35.
27. Ma H, Qazi S, Ozer Z, Zhang J, Ishkhanian R, Uckun FM. Regulatory phosphorylation of Ikaros by Bruton's tyrosine kinase. PLoS One 2013;8:e71302.
28. Díaz T, Rodríguez V, Lozano E, Mena M-P, Calderón M, Rosiñol L, et al. The BET bromodomain inhibitor CPI203 improves lenalidomide and dexamethasone activity in in vitro and in vivo models of multiple myeloma by blockade of ikaros and MYC signaling. Haematologica 2017;102:1776–84.
29. Popescu M, Gurel Z, Ronni T, Song C, Hung KY, Payne KJ, et al. Ikaros stability and pericentromeric localization are regulated by protein phosphatase 1. J Biol Chem 2009;284:13869–80.
30. Georgopoulos K. The making of a lymphocyte: the choice among disparate cell fates and the IKAROS enigma. Genes Dev 2017;31: 439–50.
31. Verbinnen I, Ferreira M, Bollen M. Biogenesis and activity regulation of protein phosphatase 1. Biochem Soc Trans 2017;45:89–99.